separations

MDPI

Supplemental Information

SI.1. System Characteristics

The full system characteristics for the MBR-MD and Baseline systems are provided in Tables S1 and S2, respectively. An influent wastewater flow of 2,500 m³/day was used for both systems.

Table S1. System characteristics for the MBR-MD system including parameters for Equations 1 and 2, DO concentrations, recycle rates, chemical dosing, membrane characteristics, feed and coolant temperatures, and UV specifications.

Module	Value	Units
Membrane Bioreactor (MBR)		
Anaerobic volume	190	m³
Anoxic volume	380	m³
Aerobic volume	1,000	m³
Aerobic DO concentration	0.20	mg/L
UF volume	140	m³
UF DO concentration	3.0	mg/L
Mixed liquor/RAS recycle rate	300	% of influent
Anoxic to anaerobic recycle rate	200	% of influent
NaClO concentration	11	mg/L
SRT	12	days
Max transmembrane pressure (TMP)	55	kPa
UF membrane type	PVDF	-
UF membrane product	Suez ZW 500M, 1M	-
Pump head	1.0	m
Pump efficiency	0.8	-
Methane emission factor	0.63	mass % of COD inf.
Nitrous oxide emission factor	0.017	mass % of TKN inf.
Dewatering power consumption	0.7	kWh/m³-sludge
Mixing power consumption	0.055	kWh/m³
Membrane Distillation (MD)		
Membrane thickness	67	μm
Membrane porosity	0.81	-
Membrane pore size	0.45	μm
Membrane area	7.2	m²
Feed temperature	80	°C
Coolant temperature	20	°C
Feed flowrate	9.1	L/min
Coolant flowrate	9.1	L/min
Ultraviolet (UV)		
UV system	Viqua S2Q-PA	-

UV dose	40	mJ/cm^2
UV power consumption	0.055	kWh/m^3

Table S2. System characteristics for the Baseline system including parameters for Equations 1, 3, and 4, DO concentration, recycle rates, chemical dosing, membrane characteristics, sizing configurations, and UV specifications.

Module	Value	Units
Conventional Treatment		
Overflow rate	36	m/day
Hydraulic retention time	2.0	hr
BOD loading rate	0.3	kg BOD/day/m^3
Estimated BOD concentration	250	mg/L
Primary clarifier volume	200	m^3
Secondary clarifier volume	200	m^3
Aeration tank volume	2,080	m^3
Aeration tank DO concentration	4.0	mg/L
RAS recycle rate	70	% of influent
FeCl$_3$ concentration	12	mg/L
SRT	6.0	days
Pump head	1.0	m
Pump efficiency	0.8	-
Methane emission factor	0.63	mass % of COD inf.
Nitrous oxide emission factor	0.017	mass % of TKN inf.
Dewatering power consumption	0.70	kWh/m^3-sludge
Mixing power consumption	0.055	kWh/m^3
Microfiltration (MF)		
MF membrane type	PVDF	-
MF membrane product	DuPont SFD-2660	-
Total trains	10	-
Modules/train	12	-
Max transmembrane pressure (TMP)	210	kPa
MF recovery	90	%
Ca(OH)$_2$ concentration	15	mg/L
Citric acid concentration	0.2	mg/L
NaOH concentration	3.6	mg/L
Reverse Osmosis (RO)		
RO membrane type	Polyamide	-
RO membrane product	DuPont BW30HR-440i	-
RO recovery	85	%
NaClO concentration	11	mg/L
H$_2$SO$_4$ concentration	24	mg/L
RO stages	5	-
RO pressure vessels/stage	2	-

RO elements/pressure vessel	7	-
Ultraviolet-Advanced Oxidation Process (UV-AOP)		
UV power consumption	0.07	kWh/m³

The system characteristics of Tables S1 and S2 were then used in the respective models to calculate the energy consumption, direct air emissions, sludge wasting, and water quality for MBR-MD and Baseline using the feed solution of Table 1. Wastewater fraction, aeration/mass transfer, kinetic, stoichiometric, settling, biofilm, and physical/chemical parameters in BioWin were all set to default values for both MBR-MD and Baseline systems.

SI.2. Air Gap MD and Baseline Modeling

The MD modeling process developed by [35] is shown schematically in Figure S1. In this model, a counter-current air gap MD process is simulated by inputting the required membrane characteristics and operating conditions (Table S1) and calculating the water flux and outlet temperatures. The model is first run by inputting a guess for the coolant outlet. The T_{guess} is then used in the model to calculate the coolant inlet—if the calculated coolant inlet ($T_{c,n}$) does not match the known coolant inlet ($T_{c,known} = 20°C$) the model is run again using an updated T_{guess} until the calculated coolant inlet is equal to the known coolant inlet.
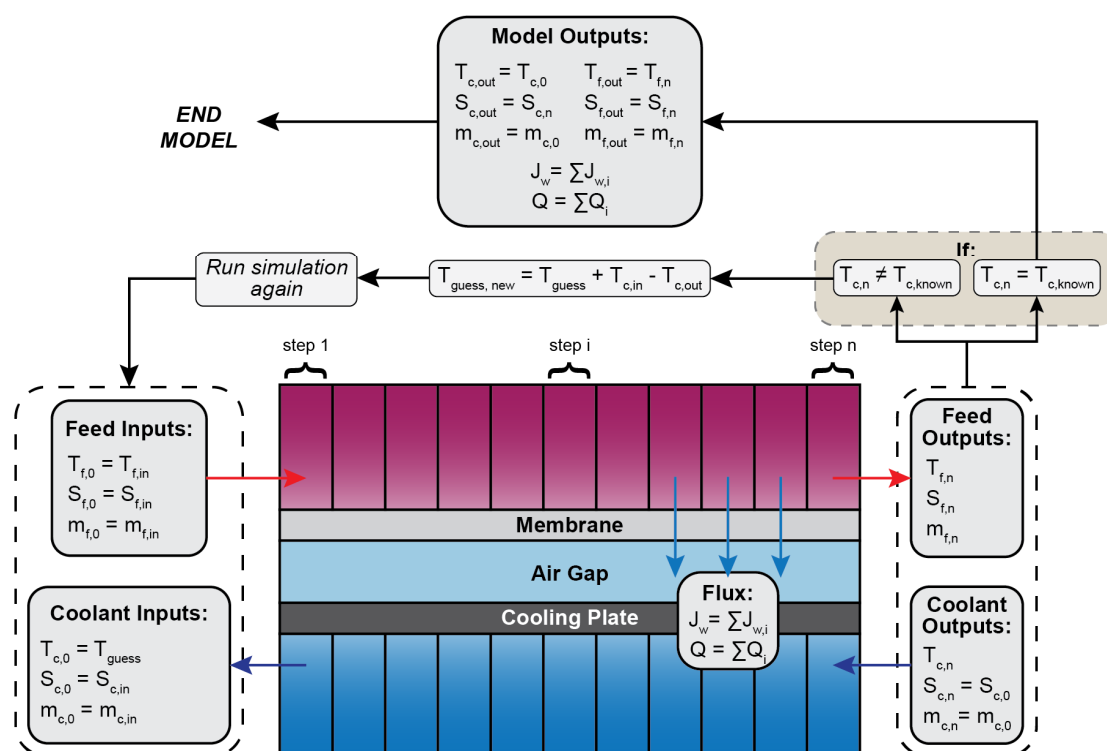
Figure S1. MD modeling process for a counter-current configuration.

Seawater property equations from [36] used for the stepwise MD model are provided in Table S3.

Table S3. Equations from [36] for the thermophysical properties of saline and pure water.

Parameter	Quality	Equation Number from [36]
Vapor Pressure	Saline	Eq. 29
	Pure	Eq. 53
Density	Saline	Eq. 5
	Pure	Eq. 50
Viscosity	Saline	Eq. 20
	Pure	Eq. 21
Specific Heat	Saline	Eq. 9
	Pure	Eq. 51
Thermal Conductivity	Saline	Eq. 13
	Pure	Eq. 52
Heat of Evaporation	Saline	Eq. 37
	Pure	Eq. 54
Specific Enthalpy	Saline	Eq. 43
	Pure	Eq. 55

The average MD rejection of ammonia, COD, nitrate, nitrite, phosphate, TN, and TOC from various references Table S4) were used to obtain the final effluent quality from the MBR-MD system.

Table S4. MD rejections for common water quality contaminants and their respective sources.

Reference	Rejection (%)						
	$NH_4 - N$	COD	$NO_3 - N$	$NO_2 - N$	$PO_4 - P$	TN	TOC
[3]	60	99.99	-		91	-	-
[4]	98.73	-	99.81	99.99	99.99	-	-
[5]	-	-	-	-	-	-	99.5
[6]	53.1	97.2	-	-	-	-	-
[7]	-	46.2	-	-	-	63.7	-
[8]	89.5	84.62	-	-	-	-	-
[9]	-	98.64	-	-	-	-	-
[10]	-	89.6	-	-	-	-	-
[11]	-	89	-	-	-	-	-
[12]	50	96	-	-	-	-	-
[13]	70	99	-	-	-	-	-

[14]	94.52	-	-	-	-	94.07	92.04
[15]	-	95.3	-	-	-	-	95.7
[16]	-	-	-	-	-	98	98
[17]	-	-	-	-	-	-	49.1
[18]	34	89.11	-	-	-	-	-
[19]	99.89	-	-	-	-	99.82	96.58
Average	72.19	89.51	99.81	99.99	95.50	88.90	88.49

In the Baseline modeling process, predicted effluent concentrations were compared to operational effluent concentrations from OCWD to validate the model for the Baseline (Table S5). Overall, results from the modeled and operational scenarios are in agreement with only slight variations in effluent water concentrations. Compared to operational data from OCWD, the modeled effluent is marginally lower in ammonia and TOC while exhibiting slightly higher concentrations for phosphate, TN, and TON [41]. These slight discrepancies could be due to the model's idealized nature and the subsequent exclusion of operational failures or issues such as MF/RO membrane fouling or scaling, pump malfunctions, or other equipment failures.

Table S5. Operational water quality data compared to modeled water quality data for the Baseline system.

Parameter	OCWD (operational)*	Baseline (modeled)
COD	7.58	7.43
NH_4-N	0.1	0.01
NO_3-N	0.67	0.70
NO_2-N	0.033	0.0038
ON	0.02	0.12
TN	0.80	0.83
PO_4-P	0.01	0.09
TOC	0.11	0.06
TSS	0	0

*Operational data obtained from the 2019 Annual GWRS Report [41].

Literature values for the available waste heat at various sized power plants (Table S6) were used to estimate what proportion of the MD energy requirements that could be met with waste heat for a hypothetical full-scale system. The LCA was run using different proportions of waste heat to determine the dependence of impacts on grid electricity use.

Table S6. Values for the amount of waste heat available from power plants found in the literature. Values were scaled to the OCWD effluent flow and the required grid energy for the MD system was subsequently calculated.

Power Plant Waste Heat (MW)	Scaled Waste Heat Available (kWh/m^3)	Required MD Grid Energy (kWh/m^3)	MD Grid Energy Percentage	LCA Scenario Name	Source
200	13.8	160	92%	MBR-92	[82]
700	48.3	125	72%	MBR-72	[45]
1,018	70.3	103	60%	MBR-60	[83]
1,364	94.2	79.5	46%	MBR-46	[84]
1,888	130	43.3	25%	MBR-MD-25	[85]
2,243	155	18.8	11%	MBR-MD-11	[86]
2,400	166	8.00	5%	MBR-MD-5	[87]
3,467	239	0	0%	MBR-MD-0	[88]

Emissions factors used to calculate the direct emissions of CH_4 and N_2O from the biotreatment by the MBR-MD and Baseline systems are shown in Table S7.

Table S7. Literature sources for the emissions factors.

Authors	N$_2$O EF (% of TKN inf.)	CH$_4$ EF (% of COD inf.)
[29]	0.0425	-
[30]	0.001	-
[31]	0.0205	-
[32]	-	0.16
[33]	-	0.08
[34]	-	0.87
[34]	-	0.53
[34]	-	1.2
[34]	-	0.8
[35]	-	0.85
[35]	-	0.7
[36]	-	1.13
[37]	0.0045	0.007
Average	0.0171	0.633

SI.3. Baseline Process Flow

The process flow diagram for the Baseline potable reuse scheme is shown in Figure S3. Wastewater is first pumped to a primary clarifier where a ferric chloride (FeCl₃) coagulant is added to promote the formation of flocs and the removal of phosphorus. These flocs then settle to the bottom of the clarifier where they are pumped out and disposed of as primary sludge. The rest of the wastewater is then sent from the top of the clarifier to an aeration basin to allow sufficient oxygen for the microorganisms in the activated sludge. The wastewater is then sent to a secondary clarifier where sedimentation occurs and the secondary sludge is wasted from the bottom. A portion of the secondary sludge is sent back to the aeration tank as the RAS recycle and the remaining is wasted. After the biological treatment, the treated wastewater is sent to the MF and RO systems for further purification. Concentrate from the RO system is disposed of offshore. As the final treatment process, the purified water is sent through a UV-AOP system to further remove any pathogenic viruses and bacteria. The final product water is of very high quality and is suitable for indirect potable reuse.
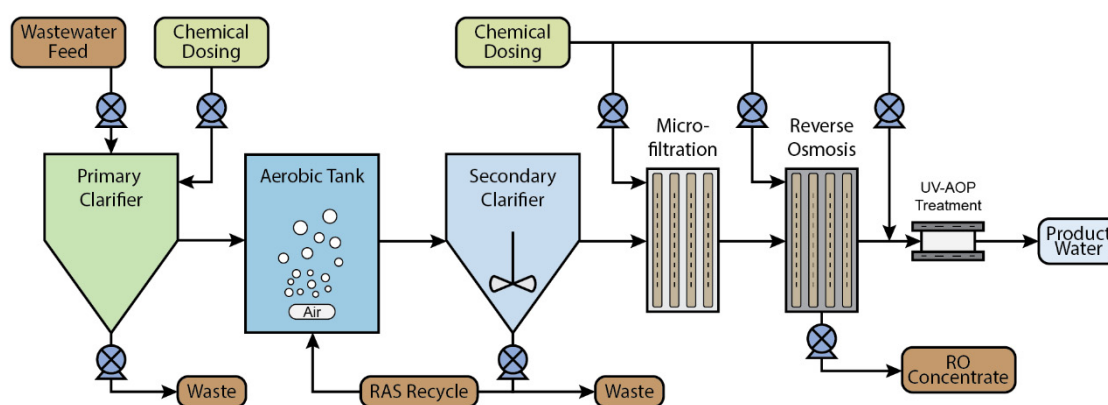

Figure S2. Process flow diagram for the Baseline system developed from OCSD and OCWD.

SI.4. Modeling Results

Results from the MBR-MD modeling are given in Table S8. These results were obtained by the modeling processes outlined in Sections 2.3.2 and 2.3.3 and by using the inputs shown in Table S1.

Table S8. MBR-MD modeling results for the MBR, MD, and UV sub-systems. Results include energy consumption, sludge wasting, recycle/effluent flow rates, and air flow rates.

Module	Value	Units
Membrane Bioreactor (MBR)		
Air flow rate	9,120*	m³/hr

Blower power	0.52[*]	kWh/m^3
RAS flow	7,410[*]	m^3/day
Anoxic to anaerobic flow	5,000[*]	m^3/day
Aerobic to anoxic flow	6,250[*]	m^3/day
Secondary solids mass	479[*]	kg/day
Secondary dewatering volume	92.7[*]	m^3/day
Dewatering power	0.027[†]	kWh/m^3
Influent pump	0.004[§]	kWh/m^3
Anoxic to anaerobic pump	0.007[§]	kWh/m^3
Aerobic to anoxic pump	0.009[§]	kWh/m^3
UF permeate pump	0.019[§]	kWh/m^3
RAS pump	0.010[§]	kWh/m^3
Effluent flow	2,420[*]	m^3/day
Membrane Distillation (MD)		
Specific thermal energy	174[**]	kWh/m^3
Feed pump	0.038[§]	kWh/m^3
Coolant pump	0.038[§]	kWh/m^3
Effluent flow	2,420[**]	m^3/day
Ultraviolet (UV)		
Specific energy consumption	0.055[††]	kWh/m^3

[*]BioWin modeling results, [†]Calculated from literature values, [§]Calculated from relevant equations in the literature, [**]MD modeling results from [35], [††]Calculated from manufacturer specifications.

The majority of the MBR energy demand is from aeration and dewatering (Table S8). Of all the pumps, the UF permeate pump has the highest energy demand, followed by the RAS and other recycle pumps. For the MD module, the STEC is significantly higher than the SEC due to pumping.

Results from the Baseline modeling are given in Table S9. These results were obtained by the modeling processes outlined in Section 2.3.4 and by using the inputs shown in Table S2.

Table S9. Baseline modeling results for the conventional treatment, MF, RO, and UV sub-systems. Results include energy consumption, sludge wasting, recycle/effluent flow rates, and air flow rates.

Module	Value	Units
Conventional Treatment		
Air flow rate	2,450[*]	m^3/hr
Blower power	0.403[*]	kWh/m^3
RAS flow	1,670[*]	m^3/day
Primary solids mass	461[*]	kg/day
Secondary solids mass	147[*]	kg/day

Primary dewatering volume	25[*]	m^3/day
Secondary dewatering volume	79.8[*]	m^3/day
Dewatering power	0.030[†]	kWh/m^3
Effluent flow	2,420[*]	m^3/day
Influent pump	0.004[§]	kWh/m^3
Chemical pump	5.70e-7[§]	kWh/m^3
Primary solids pump	5.50e-6[§]	kWh/m^3
RAS pump	2.46e-3[§]	kWh/m^3
Effluent pump	3.40e-3[§]	kWh/m^3
Microfiltration (MF)		
Influent pump	0.171[§§]	kWh/m^3
Cleaning in place pump	9.3e-3[§§]	kWh/m^3
Backwashing pump	0.092[§§]	kWh/m^3
Air scour pump	2.1e-3[§§]	kWh/m^3
Effluent flow	2,160[§§]	m^3/day
Reverse Osmosis (RO)		
Specific energy	1.08[§§]	kWh/m3
RO concentrate	324[§§]	m^3/day
Effluent flow	1,840[§§]	m^3/day
Ultraviolet-Advanced Oxidation Process (UV-AOP)		
UV power consumption	0.070[†]	kWh/m^3

[*]BioWin modeling results, [†]Calculated from literature values, [§]Calculated from relevant equations in the literature, [††]Calculated from manufacturer specifications, [§§]WAVE modeling results.

Similar to the MBR, a majority of the conventional treatment energy demand is from aeration and dewatering. Of all the pumps in the conventional treatment process, the influent pump has the highest energy demand. This is also true for the UF system where the influent pump accounts for more than 65% of the total pumping energy demand.

SI.5. Environmental Impact Results

Environmental impact results for the Baseline (Figure S3) and MBR-MD-0 (Figure S4) are shown below.
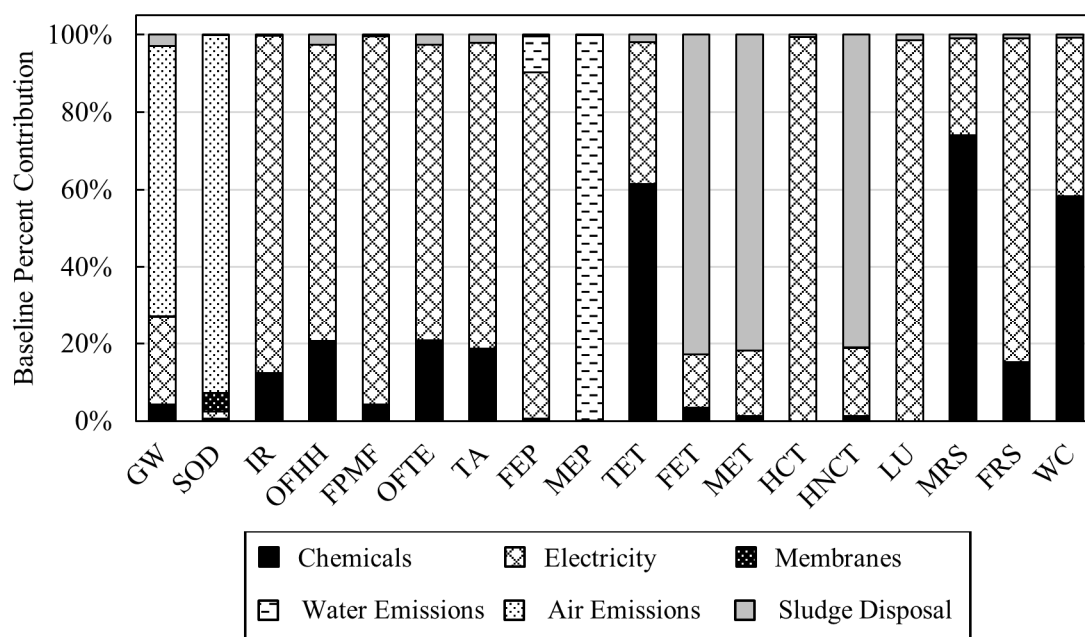
Figure S3. Percentage contributions to each impact category for the Baseline system.
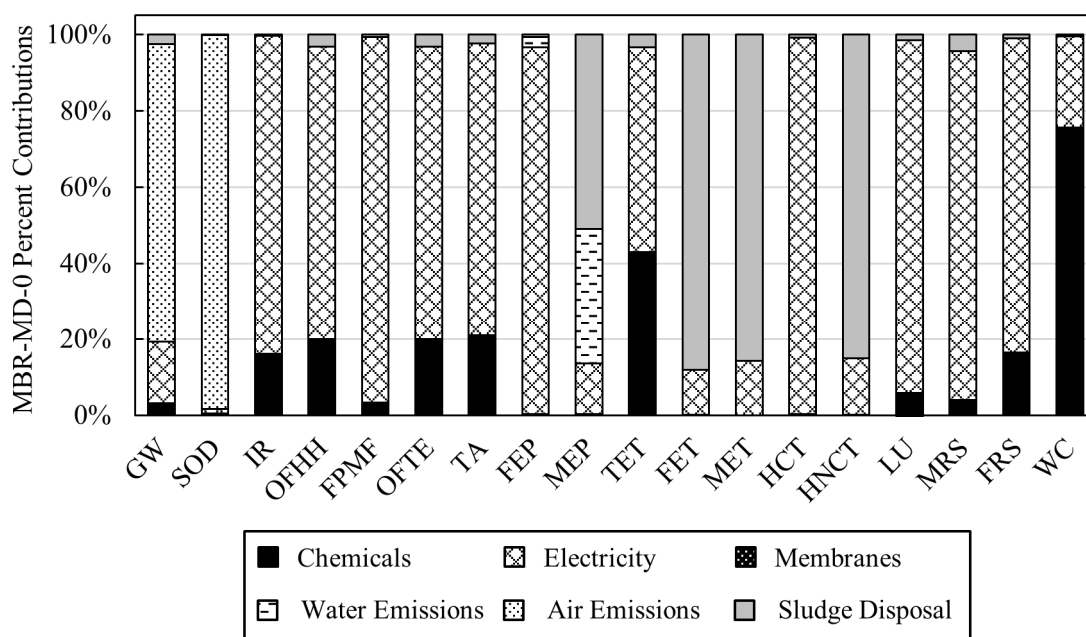

Figure S4. Percentage contributions to each impact category for the MBR-MD-0 scenario of the MBR-MD system when 100% waste heat is used for MD energy requirements.

Environmental impact results for the MBR-MD-11 (11% of MD heat supplied from the electrical grid) and MBR-MD-25 (25% of MD heat supplied from electrical grid) are show below. In the MBR-MD-5 scenario (Figure S5), each impact category except for SOD and MEP has a higher environmental impact compared to the Baseline. These increased impacts are due entirely to the increased grid energy consumption by

the MD module. Increasing the MD grid energy percentage to 25% (Fig. S6) results in even larger environmental impacts compared to the Baseline. The largest impact category in the MBR-MD-25 scenario is HCT, with an impact greater than 2,800% of the Baseline. Several other impact categories display impacts greater than 1,000% of the Baseline. For the MBR-MD-25 scenario, SOD and MEP are the only impact categories where the total impacts are less than the Baseline and electricity consumption is not the largest contributor.

Figure S5. Percentage contributions to each impact category for the MBR-MD-11 scenario of the MBR-MD system scaled to the Baseline system. The dashed line represents 100% as a comparison to the Baseline.
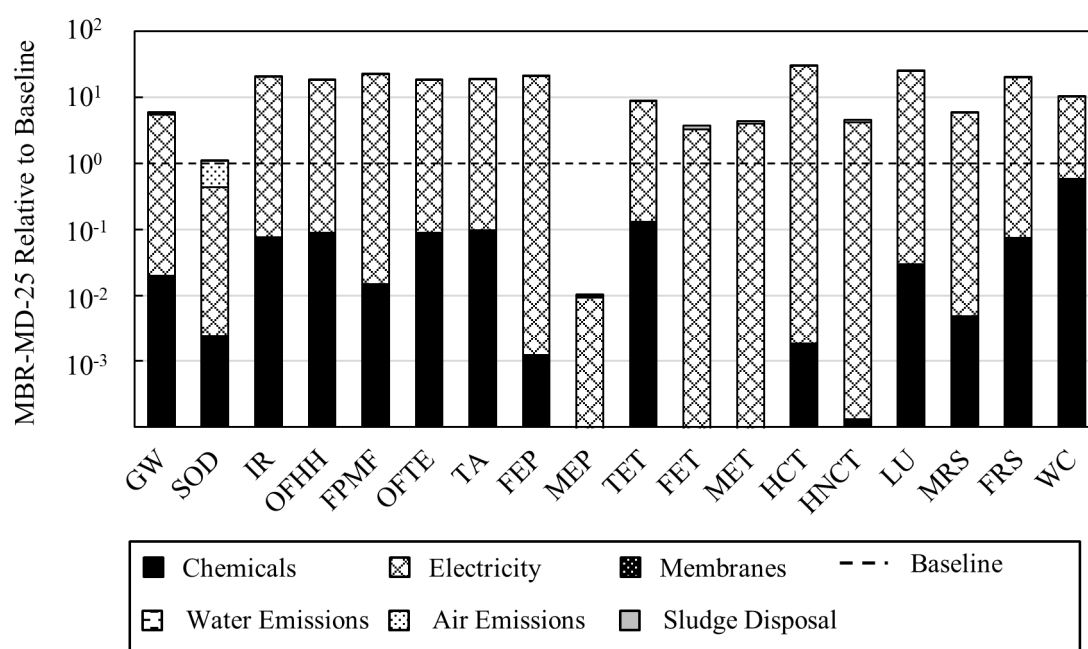
Figure S6. Percentage contributions to each impact category for the MBR-MD-25 scenario of the MBR-MD system scaled to the Baseline system. The dashed line represents 100% as a comparison to the Baseline [20–22,35,36,41,45,77–106].

SI.6. References

35.   Noamani, S.; Niroomand, S.; Rastgar, M.; Azhdarzadeh, M.; Sadrzadeh, M. Modeling of Air-Gap Membrane Distillation and Comparative Study with Direct Contact Membrane Distillation. *Ind. Eng. Chem. Res.* **2020**, *59*, 21930–21947, doi:10.1021/ACS.IECR.0C04464/SUPPL_FILE/IE0C04464_SI_001.PDF.

36.   Sharqawy, M.H.; Lienhard V, J.H.; Zubair, S.M. Thermophysical Properties of Seawater: A Review of Existing Correlations and Data. *Desalin. Water Treat.* **2010**, *16*, 354–380, doi:10.5004/DWT.2010.1079.

21.   Song, X.; Luo, W.; McDonald, J.; Khan, S.J.; Hai, F.I.; Price, W.E.; Nghiem, L.D. An Anaerobic Membrane Bioreactor – Membrane Distillation Hybrid System for Energy Recovery and Water Reuse: Removal Performance of Organic Carbon, Nutrients, and Trace Organic Contaminants. *Sci. Total Environ.* **2018**, *628–629*, 358–365, doi:10.1016/J.SCITOTENV.2018.02.057.

77.   Volpin, F.; Jiang, J.; El Saliby, I.; Preire, M.; Lim, S.; Hasan Johir, M.A.; Cho, J.; Han, D.S.; Phuntsho, S.; Shon, H.K. Sanitation and Dewatering of Human Urine via Membrane Bioreactor and Membrane Distillation and Its Reuse for Fertigation. *J. Clean. Prod.* **2020**, *270*, 122390, doi:10.1016/J.JCLEPRO.2020.122390.

78.   Nguyen, N.C.; Nguyen, H.T.; Chen, S.S.; Ngo, H.H.; Guo, W.; Chan, W.H.; Ray, S.S.; Li, C.W.; Hsu, H. Te A Novel Osmosis Membrane Bioreactor-Membrane Distillation Hybrid System for Wastewater Treatment and Reuse. *Bioresour. Technol.* **2016**, *209*, 8–15, doi:10.1016/j.biortech.2016.02.102.

89.   Jacob, P.; Phungsai, P.; Fukushi, K.; Visvanathan, C. Direct Contact Membrane Distillation for Anaerobic Effluent Treatment. *J. Memb. Sci.* **2015**, *475*, 330–339, doi:10.1016/J.MEMSCI.2014.10.021.

99.   Tibi, F.; Guo, J.; Ahmad, R.; Lim, M.; Kim, M.; Kim, J. Membrane Distillation as Post-Treatment for Anaerobic Fluidized Bed Membrane Bioreactor for Organic and Nitrogen Removal. *Chemosphere* **2019**, *234*, 756–762, doi:10.1016/J.CHEMOSPHERE.2019.06.043.

100. Kwon, D.; Bae, W.; Kim, J. Hybrid Forward Osmosis/Membrane Distillation Integrated with Anaerobic Fluidized Bed Bioreactor for Advanced Wastewater Treatment. *J. Hazard. Mater.* **2021**, *404*, 124160, doi:10.1016/J.JHAZMAT.2020.124160.

20. Shirazi, M.M.A.; Bazgir, S.; Meshkani, F. A Novel Dual-Layer, Gas-Assisted Electrospun, Nanofibrous SAN4-HIPS Membrane for Industrial Textile Wastewater Treatment by Direct Contact Membrane Distillation (DCMD). *J. Water Process Eng.* **2020**, *36*, 101315, doi:10.1016/J.JWPE.2020.101315.

101. Mokhtar, N.M.; Lau, W.J.; Ismail, A.F.; Kartohardjono, S.; Lai, S.O.; Teoh, H.C. The Potential of Direct Contact Membrane Distillation for Industrial Textile Wastewater Treatment Using PVDF-Cloisite 15A Nanocomposite Membrane. *Chem. Eng. Res. Des.* **2016**, *111*, 284–293, doi:10.1016/J.CHERD.2016.05.018.

106. Li, F.; Huang, J.; Xia, Q.; Lou, M.; Yang, B.; Tian, Q.; Liu, Y. Direct Contact Membrane Distillation for the Treatment of Industrial Dyeing Wastewater and Characteristic Pollutants. *Sep. Purif. Technol.* **2018**, *195*, 83–91, doi:10.1016/J.SEPPUR.2017.11.058.

103. Davey, C.J.; Liu, P.; Kamranvand, F.; Williams, L.; Jiang, Y.; Parker, A.; Tyrrel, S.; McAdam, E.J. Membrane Distillation for Concentrated Blackwater: Influence of Configuration (Air Gap, Direct Contact, Vacuum) on Selectivity and Water Productivity. *Sep. Purif. Technol.* **2021**, *263*, 118390, doi:10.1016/J.SEPPUR.2021.118390.

104. Zoungrana, A.; Zengin, İ.H.; Elcik, H.; Özkaya, B.; Çakmakci, M. The Treatability of Landfill Leachate by Direct Contact Membrane Distillation and Factors Influencing the Efficiency of the Process. *Desalin. WATER Treat.* **2017**, *71*, 233–243, doi:10.5004/DWT.2017.20494.

79. Zhou, Y.; Huang, M.; Deng, Q.; Cai, T. Combination and Performance of Forward Osmosis and Membrane Distillation (FO-MD) for Treatment of High Salinity Landfill Leachate. *Desalination* **2017**, *420*, 99–105, doi:10.1016/J.DESAL.2017.06.027.

102. Wu, Y.; Kang, Y.; Zhang, L.; Qu, D.; Cheng, X.; Feng, L. Performance and Fouling Mechanism of Direct Contact Membrane Distillation (DCMD) Treating Fermentation Wastewater with High Organic Concentrations. *J. Environ. Sci. (China)* **2018**, *65*, 253–261, doi:10.1016/J.JES.2017.01.015.

22. Luo, W.; Phan, H. V.; Li, G.; Hai, F.I.; Price, W.E.; Elimelech, M.; Nghiem, L.D. An Osmotic Membrane Bioreactor-Membrane Distillation System for Simultaneous Wastewater Reuse and Seawater Desalination: Performance and Implications. *Environ. Sci. Technol.* **2017**, *51*, 14311–14320, doi:10.1021/acs.est.7b02567.

80. Han, L.; Tan, Y.Z.; Netke, T.; Fane, A.G.; Chew, J.W. Understanding Oily Wastewater Treatment via Membrane Distillation. *J. Memb. Sci.* **2017**, *539*, 284–294, doi:10.1016/J.MEMSCI.2017.06.012.

105. Ali Zoungrana; Ismail Zengin; Dogan Karadag; Mehmet Cakmakci Treatability of Municipal Wastewater with Direct Contact Membrane Distillation Sigma Journal of Engineering and Natural Sciences. *Sigma J. Eng. Nat. Sci.* **2017**, *8*, 245–254.

81. Lu, D.; Liu, Q.; Zhao, Y.; Liu, H.; Ma, J. Treatment and Energy Utilization of Oily Water via Integrated Ultrafiltration-Forward Osmosis–Membrane Distillation (UF-FO-MD) System. *J. Memb. Sci.* **2018**, *548*, 275–287, doi:10.1016/J.MEMSCI.2017.11.004.

41. Orange County Water District Groundwater Replenishment System 2019 Annual Report. **2020**.

82. Mikielewicz, D.; Wajs, J.; Ziółkowski, P.; Mikielewicz, J. Utilisation of Waste Heat from the Power Plant by Use of the ORC Aided with Bleed Steam and Extra Source of Heat. *Energy* **2016**, *97*, 11–19, doi:10.1016/J.ENERGY.2015.12.106.

45. Dow, N.; Gray, S.; Li, J. de; Zhang, J.; Ostarcevic, E.; Liubinas, A.; Atherton, P.; Roeszler, G.; Gibbs, A.; Duke, M. Pilot Trial of Membrane Distillation Driven by Low Grade Waste Heat: Membrane Fouling and Energy Assessment. *Desalination* **2016**, *391*, 30–42, doi:10.1016/J.DESAL.2016.01.023.

83. Tai, C.; Tian, G.; Lei, W. A Water-Heat Combined Supply System Based on Waste Heat from a Coastal Nuclear Power Plant in Northern China. *Appl. Therm. Eng.* **2022**, *200*, 117684, doi:10.1016/J.APPLTHERMALENG.2021.117684.

84. Su, Z.; Yang, L. A Novel and Efficient Cogeration System of Waste Heat Recovery Integrated Carbon Capture and Dehumidification for Coal-Fired Power Plants. *Energy Convers. Manag.* **2022**, *255*, 115358, doi:10.1016/J.ENCONMAN.2022.115358.

85. Fathi, N.; McDaniel, P.; Aleyasin, S.S.; Robinson, M.; Vorobieff, P.; Rodriguez, S.; Oliveira, C. de Efficiency Enhancement of Solar Chimney Power Plant by Use of Waste Heat from Nuclear Power Plant. *J. Clean. Prod.* **2018**, *180*, 407–416, doi:10.1016/J.JCLEPRO.2018.01.132.

86. Obara, S.; Tanaka, R. Waste Heat Recovery System for Nuclear Power Plants Using the Gas Hydrate Heat Cycle. *Appl. Energy* **2021**, *292*, 116667, doi:10.1016/J.APENERGY.2021.116667.

87. Wealer, B.; Bauer, S.; Landry, N.; Seiß, H.; von Hirschhausen DIW Berlin, C. Navigating the Roadmap for Clean, Secure and Efficient Energy Innovation: Nuclear Power Reactors Worldwide-Tech-Nology Developments, Diffusion Patterns, and Country-by-Country Analysis of Imple-Mentation (1951-2017). **2019**.

88. Yu, M.G.; Nam, Y. Feasibility Assessment of Using Power Plant Waste Heat in Large Scale Horticulture Facility Energy Supply Systems. *Energies 2016, Vol. 9, Page 112* **2016**, *9*, 112, doi:10.3390/EN9020112.

91. Czepiel, P.; Crill, P.; Harriss, R. Nitrous Oxide Emissions from Municipal Wastewater Treatment. *Environ. Sci. Technol.* **1995**, *29*, 2352–2356, doi:10.1021/ES00009A030/ASSET/ES00009A030.FP.PNG_V03.

92. Sümer, E.; Weiske, A.; Benckiser, G.; Ottow, J.C.G. Influence of Environmental Conditions on the Amount of N2O Released from Activated Sludge in a Domestic Waste Water Treatment Plant. *Experientia* **1995**, *51*, 419–422, doi:10.1007/BF01928908.

93. Benckiser, G.; Eilts, R.; Linn, A.; Lorch, H.J.; Sümer, E.; Weiske, A.; Wenzhöfer, F. N2O Emissions from Different Cropping Systems and from Aerated, Nitrifying and Denitrifying Tanks of a Municipal Waste Water Treatment Plant. *Biol. Fertil. Soils 1996 233* **1996**, *23*, 257–265, doi:10.1007/BF00335953.

90. Czepiel, P.M.; Crill, P.M.; Harriss, R.C. Methane Emissions from Municipal Wastewater Treatment Processes. *Environ. Sci. Technol.* **1993**, *27*, 2472–2477, doi:10.1021/ES00048A025/ASSET/ES00048A025.FP.PNG_V03.

94. Wang, J.; Zhang, J.; Xie, H.; Qi, P.; Ren, Y.; Hu, Z. Methane Emissions from a Full-Scale A/A/O Wastewater Treatment Plant. *Bioresour. Technol.* **2011**, *102*, 5479–5485, doi:10.1016/J.BIORTECH.2010.10.090.

95. STOWA Emissies van Broeikasgassen van Rwzi's.

96. VROM Protocol 8136 Afvalwater, t.b.v NIR 2008 Uitgave Maart 2008 6B: CH4 En N2O Uit Afvalwater, The Hague, Netherlands.

97. Daelman, M.R.J.; van Voorthuizen, E.M.; van Dongen, U.G.J.M.; Volcke, E.I.P.; van Loosdrecht, M.C.M. Methane Emission during Municipal Wastewater Treatment. *Water Res.* **2012**, *46*, 3657–3670, doi:10.1016/J.WATRES.2012.04.024.

98. Tumendelger, A.; Alshboul, Z.; Lorke, A. Methane and Nitrous Oxide Emission from Different Treatment Units of Municipal Wastewater Treatment Plants in Southwest Germany. *PLoS One* **2019**, *14*, e0209763, doi:10.1371/JOURNAL.PONE.0209763.